# Characterization of Foam-Assisted Water-Gas Flow via Inverse Uncertainty Quantification Techniques

Gabriel Brandão de Miranda[1,2][0000−0002−2879−9040], Luisa Silva Ribeiro[1,2][0000−0001−6753−6342], Juliana Maria da Fonseca Façanha[3][0000−0002−6799−3591], Aurora Pérez-Gramatges[3,4][0000−0001−5951−6130], Bernardo Martins Rocha[1,2][0000−0002−0508−8959], Grigori Chapiro[1,2][0000−0003−4568−834X], and Rodrigo Weber dos Santos[1,2][0000−0002−0633−1391]

[1] Graduate Program in Computational Modeling, Federal University of Juiz de Fora, Juiz de Fora, Brazil
[2] Laboratory of Applied Mathematics (LAMAP), Federal University of Juiz de Fora, Juiz de Fora, Brazil
[3] Laboratory of Physical-Chemistry of Surfactants (LASURF), Pontifical Catholic University of Rio de Janeiro, Rio de Janeiro, Brazil
[4] Chemistry Department, Pontifical Catholic University of Rio de Janeiro, Rio de Janeiro, Brazil

**Abstract.** In enhanced oil recovery (EOR) processes, foam injection reduces gas mobility and increases apparent viscosity, thus increasing recovery efficiency. The quantification of uncertainty is essential in developing and evaluating mathematical models. In this work, we perform uncertainty quantification (UQ) of two-phase flow models for foam injection using the STARS model with data from a series of foam quality-scan experiments. We first performed the parameter estimation based on three datasets of foam quality-scans on Indiana limestone carbonate core samples. Then distributions of the parameters are inferred via the Markov Chain Monte Carlo method (MCMC). This approach allows propagating parametric uncertainty to the STARS apparent viscosity model. In particular, the framework for UQ allowed us to identify how the lack of experimental data affected the reliability of the calibrated models.

**Keywords:** Uncertainty Quantification · Foam Dynamics · Bayesian Inference

## 1 Introduction

Oil extraction, the process by which usable oil is extracted and removed from underground, can be divided into three categories [5]. The first category is the primary oil recovery, which raises the reservoir pressure so that recovery occurs spontaneously. This process does not have a good yield since, on average, it recovers only 30% of the original volume of oil present in the reservoir. The

ICCS Camera Ready Version 2022
To cite this paper please use the final published version:
DOI: 10.1007/978-3-031-08760-8_26

secondary oil recovery uses techniques such as injection water or gas into the reservoir through an injection well to push the oil out of the rock pores. The third category, also called enhanced oil recovery (EOR), uses more complex techniques such as thermal recovery (heating the oil to decrease its viscosity) and chemical recovery such as foam injection to reduce gas mobility and increase recovery.

EOR techniques have been increasingly used in the upstream oil industry, and in particular, one of the methods that stand out the most is foam injection. The alternating water and gas injection (WAG) process can be improved by using foams to reduce gas mobility, increase apparent viscosity, and improve recovery efficiency.

Several physical models of foam flow in porous media are available in literature [1, 10, 19]. Modeling of foam flow dynamics in porous media is very complex due to its non-Newtonian nature, its dependence on the foam texture, and the complex bubble generation/destruction process. In this work, the simplified version of the CMG-STARS model [6] is studied.

The process of estimating the model parameters is not straightforward, and several methods to this end have been proposed so far [3, 11, 12, 18]. In [3] a manual process was used to adjust the foam flow parameters to apparent viscosity data. The proposed procedure works separately with data in the low and high-quality regimes and is based on the foam quality and apparent viscosity relation. The work of [11] used data weighting and constraints when employing nonlinear least-squares minimization methods for parameter estimation. The work of [12] used a combined approach with a graphical method and least-squares minimization techniques. In [18] the problem of fitting many parameters was replaced by a procedure based on linear regression and single-variable optimization, which avoids problems related to non-unique solutions and sensitivity issues of the initial estimates. It is important to remark that these methods did not perform any uncertainty quantification after estimating the parameters. To reduce the non-uniqueness and uncertainty of solutions, the work of [2] proposes an assisted/automated method to adjust the parameters of relative permeability measurements and provides a framework for a consistent uncertainty assessment of relative permeability measurements.

The present work used Bayesian inference techniques for parameter estimation, followed by uncertainty propagation to evaluate the uncertainties associated with the foam injection process numerically. The probability distributions of the parameters were estimated using the Markov Chain Monte Carlo (MCMC) method, which seeks to find the posterior distribution of the parameters given a dataset and a prior characterization of the parameters. In particular, we assessed the distributions of the parameters using data from a series of foam quality-scan experiments to characterize the parameters better.

The remaining of this manuscript is organized as follows: in section 2 the experimental setup, the recorded data, and the methods used for parameter inference are reported; section 3 presents the results obtained in terms of least-squares methods and Bayesian methods; and section 4 ends this work with some conclusions and discussions.

ICCS Camera Ready Version 2022
To cite this paper please use the final published version:
DOI: 10.1007/978-3-031-08760-8_26

## 2 Methods

This work uses Bayesian inference techniques for parameter estimation, also known as inverse uncertainty quantification (UQ). After this first step, uncertainty propagation or forward UQ is performed to evaluate the uncertainties associated with the numerical modeling of Enhanced Oil Recovery (EOR) based on the process of coinjection of foam. This section explains the experimental setup, the recorded data, and the methods used for parameter inference.

### 2.1 Experimental Setup

The experiments used in this work were described in [7], and part of the data was used in [16]. For clarity, the setup is briefly described here. Brine prepared by dissolving adequate amounts of salt in distilled water was used in the core-flooding. The concentrations are shown in Table 1. Before preparing the surfactant solution, the brine was degassed using a vacuum pump. The salts that were used to prepare the brine were purchased from Sigma-Aldrich Brasil and were reagent grade.

Table 1: Ionic composition of injection water (IW)

| **Ions** | $Na^+$ | $K^+$ | $Ca^{2+}$ | $Mg^{2+}$ | $SO_4^{2-}$ | $Cl^-$ |
|---|---|---|---|---|---|---|
| **Concentration** (mg/L) | 11008 | 393 | 132 | 152 | 41 | 17972 |

The surfactant chosen to perform the foam injection was sodium alpha-olefin sulfonate (Bioterge AS-40), which Stepan Brasil donated. It was used at a concentration of 0.1 wt%, with a critical micellar concentration (CMC) in IW at 20º and ambient pressure conditions 0.0017 wt%. Nitrogen (99.992% purity, Linde Brasil) was used for the gas phase.

A series of three foam quality-scan experiments were performed on a sample of Indiana limestone (Kocurek Industries, USA), which was the rock used in the experiments. The dimensions and petrophysical properties of the core used in this work are presented in Table 2.

The core was loaded onto the Hassler core support under confining pressure of 3.44 MPa (500 psi) vertically. It was aspirated for two hours and then saturated under vacuum with IW. Confinement pressure and pore pressure were increased simultaneously to 17.2 MPa (2500 psi) and 13.8 MPa (2000 psi), respectively. The core sample was left at this pressure for 24 hours to saturate the core fully. Afterward, the pore pressure was decreased to 10 MPa (1500 psi), and then the brine permeability was measured. This procedure was done by injecting IW at different flow rates for pore volumes. After performing the permeability measurement, 0.1 wt%AOS surfactant solution was injected (all experiments used the same surfactant concentrations) and then through the core for at least 5 pore volumes (PV) to displace IW. The system temperature was raised to 60°C.

ICCS Camera Ready Version 2022
To cite this paper please use the final published version:
DOI: 10.1007/978-3-031-08760-8_26

Table 2: Dimensions and petrophysical properties of Indiana limestone, where $L$, $D$, $PV$, $\varphi$, and $K$ are the length, diameter, pore volume, porosity, and permeability, respectively.

| **Properties** | **Experiment 1** | **Experiment 2** | **Experiment 3** |
|---|---|---|---|
| L [m] | 0.150 | 0.150 | 0.150 |
| D [m] | 0.0382 | 0.0382 | 0.0382 |
| PV [$10^{-6} m^3$] | 26.7 | 26.7 | 27.76 |
| $\varphi$ [-] | 0.155 | 0.155 | 0.161 |
| k [$m^2$] | 2.70 $\times 10^{-13}$ | 1.57 $\times 10^{-13}$ | 2.91 $\times 10^{-13}$ |
| v[m/s] | 1.45 $\times 10^{-5}$ | 1.45 $\times 10^{-5}$ | 2.40 $\times 10^{-5}$ |

As the pressure and temperature were constant and there was no possibility of leakage, the nitrogen solution and surfactant were co-injected at constant superficial velocity ($1.45 \times 10^{-5}$ m/s) and injection flow rate (0.967 mL/min), but at different gas/liquid ratios. In Figure 1 it is possible to see the schematic drawing of core-flood apparatus used for foam injection.

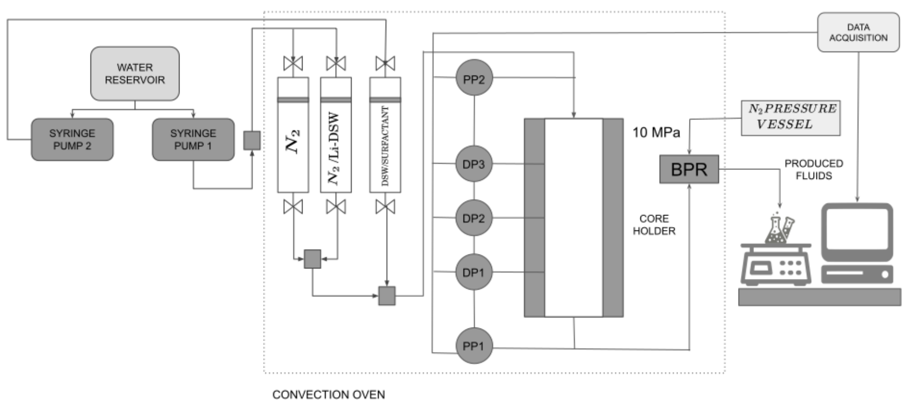


Fig. 1: Schematic drawing of core-flood apparatus.

## 2.2 Relative Permeabilities

Relative permeabilities were described by the Corey model for the two-phase flow of water and gas without surfactant, which are given by:

$$k_{rw} = k_{rw}^0 \left( \frac{S_w - S_{wc}}{1 - S_{wc} - S_{gr}} \right)^{n_w}, \quad \text{and} \quad k_{rg} = k_{rg}^0 \left( \frac{S_g - S_{gr}}{1 - S_{wc} - S_{gr}} \right)^{n_g}, \quad (1)$$

where $n_w$ and $n_g$ are the Corey exponents for water and gas, respectively, $k_{rw}^0$ and $k_{rg}^0$ are the end-point relative permeabilities for water and gas, respectively,

ICCS Camera Ready Version 2022
To cite this paper please use the final published version:
DOI: 10.1007/978-3-031-08760-8_26

$S_{wc}$ is the connate water saturation, and $S_{gr}$ the residual gas saturation. Relative permeability data for high permeability Indiana Limestone found in the literature [13] were considered. The Corey parameters used in this work, which were fitted to the relative permeability data of [13] using the techniques described in [17], are given in Table 3.

| Parameters | $S_{wc}$ | $S_{gr}$ | $n_w$ | $n_w$ | $k_{rw}^0$ | $k_{rg}^0$ |
|---|---|---|---|---|---|---|
| Values | 0.4 | 0.293 | 2.98 | 0.96 | 0.302 | 0.04 |

Table 3: Relative permeability parameters for datasets.

### 2.3 STARS Model

To model the two-phase flow for foam flow, the CMG-STARS mathematical model [6] was used. In this model the foam effects are modeled considering a reduction factor that affects the mobility of the gas phase. The mobility reduction factor ($MRF$) term can describe the effects of surfactant concentration, water and oil saturations, shear-thinning, and other effects.

Let the mobility of gas and water phases be denoted by $\lambda_g$ and $\lambda_w$, respectively. The total mobility $\lambda_T$ is defined as $\lambda_T = \lambda_w + \lambda_g$. Thus, the apparent viscosity can be defined as the inverse of total relative mobility:

$$\mu_{app} = \lambda_T^{-1} = \left(\lambda_w + \frac{\lambda_g}{MRF}\right)^{-1}, \tag{2}$$

where the fact that mobility of the gas phase is influenced by the foam through the mobility reduction factor $MRF$ is already taken into account.

The fractional gas flow is then redefined as follows including the MRF function:

$$f_g = \frac{\lambda_g}{MRF\left(\lambda_w + \frac{\lambda_g}{MRF}\right)} = \frac{\lambda_g}{MRF}\mu_{app}. \tag{3}$$

The gas mobility is given by:

$$\lambda_g = \frac{k_{rg}}{MRF\mu_g}, \quad MRF = 1 + fmmobF_2, \tag{4}$$

where the $F_2$ term describes the effects of water saturation, and is given by:

$$F_2 = \frac{1}{2} + \frac{1}{\pi}arctan(sfbet(S_w - SF)), \tag{5}$$

where $fmmob$, $sfbet$, and $SF$ are model parameters.

ICCS Camera Ready Version 2022
To cite this paper please use the final published version:
DOI: 10.1007/978-3-031-08760-8_26

### 2.4 Procedures for Parameter Estimation

Two approaches were used in this work for parameter estimation: nonlinear least-squares minimization and Bayesian inference. To estimate parameters with nonlinear least-squares we used the Differential Evolution (DE) method implemented in the `lmfit` library [14] available in the Python programming language.

For Bayesian inference of the distributions of the parameters, the Markov Chain Monte Carlo (MCMC) [4] method was used. The prior distributions of the parameters of the model required for the MCMC were chosen considering the physical ranges of the parameters and knowledge available in the literature [8]. The `PyMC3` library [15] for Bayesian modeling was used for executing the MCMC method. For the inference process, four chains are built independently. The univariate slice sampler was adopted as the step function, $10^4$ samples were drawn for each randomized parameter, and $10^3$ samples were discarded from each of the final chains. The joint of these four chains describes a sample of the posterior distribution for each parameter.

Assuming $\theta$ as parameters of the STARS model and $D$ as the data set, the MCMC attempts to estimate:

$$\mathbb{P}(D|\theta) = \frac{\mathbb{P}(D|\theta)\mathbb{P}(\theta)}{\mathbb{P}(D)} \tag{6}$$

where $\mathbb{P}(\theta)$ represents the prior knowledge of the input parameters $\theta$, as a joint probability distribution; $\mathbb{P}(D|\theta)$ is the likelihood function; and $\mathbb{P}(D)$ is the evidence, a normalization factor for the posterior distribution.

To carry out the MCMC estimation, our prior knowledge about the parameters' distributions must be provided. Table 4 summarizes the priors adopted in this work, which was based on the choice used in previous works [16].

Table 4: Chosen prior distributions for the parameters of the CMG-STARS foam model used in the MCMC method.

| fmmob | SF | sfbet |
|---|---|---|
| $\mathcal{U}(10, 1000)$ | $\mathcal{U}(S_{wc}, 1 - S_{gr})$ | $\mathcal{U}(10, 1000)$ |

### 2.5 Sensitivity Analysis

A variance based sensitivity analysis was used to assess how the input parameters $x_i \in \theta$ and their interactions contribute to the variations of any quantity of interest $\mathcal{Y}$. The main and total Sobol indices were used to this end. The first-order Sobol index, presented in the equation 7, expresses how any uncertain input $x_i$ directly contributes to the variance of the output $\mathcal{Y}$.

$$S_i = \frac{\mathbb{V}[\mathbb{E}[\mathcal{Y}|x_i]]}{\mathbb{V}[\mathcal{Y}]} \tag{7}$$

ICCS Camera Ready Version 2022
To cite this paper please use the final published version:
DOI: 10.1007/978-3-031-08760-8_26

To estimate the changes in $\mathbb{V}[\mathcal{Y}]$ considering the first and high order interactions of the $i$-th uncertain entry, the total Sobol index is evaluated. It is given by:

$$S_{T_i} = 1 - \frac{\mathbb{V}[\mathbb{E}[\mathcal{Y}|x_{-i}]]}{\mathbb{V}[\mathcal{Y}]} \tag{8}$$

where $x_{-1}$ denotes the set of all input parameters except $x_i$. The sensitivity indices were computed with the `SAlib` library using the Saltelli method [9]. Bounds for parameters in the SA were defined as the bounds from the 90% confidence interval of the marginal posterior distributions.

## 3 Results

### 3.1 Least-Squares estimates

First, we present some parameter estimates obtained with the nonlinear least-squares method to first characterize the foam flow in the core-flooding experiments. Figure 2 shows the results of the foam quality scan experiment in terms of the pressure drop versus time.

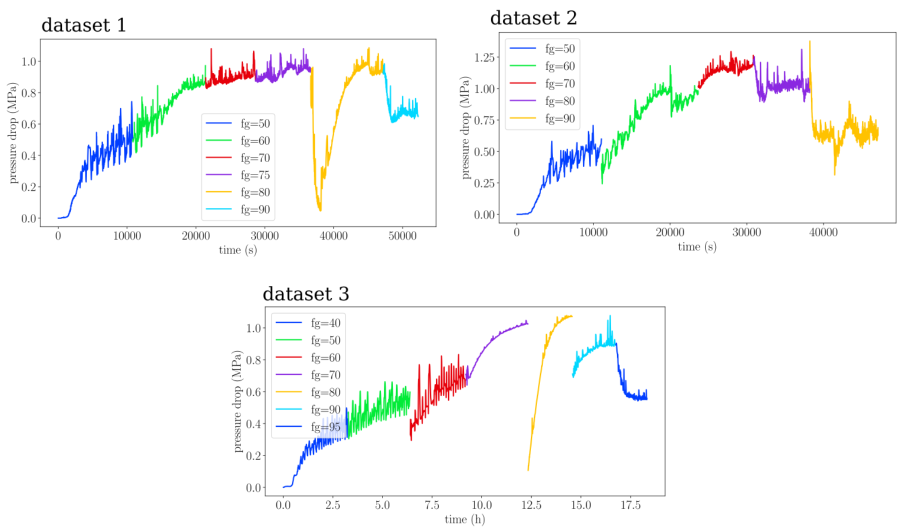


Fig. 2: Foam quality-scan experiment results

Figure 3 shows the steady-state experimental data for apparent viscosity as a function of foam quality for the three experiments previously described in Table 2. Fittings of the STARS model to the corresponding data for each dataset are also shown in Figure 3. Model fittings and data for experiments #01, #02, and #03 are represented by blue, orange, and green, respectively, where dots represent the data and solid lines model evaluations.

ICCS Camera Ready Version 2022
To cite this paper please use the final published version:
DOI: 10.1007/978-3-031-08760-8_26

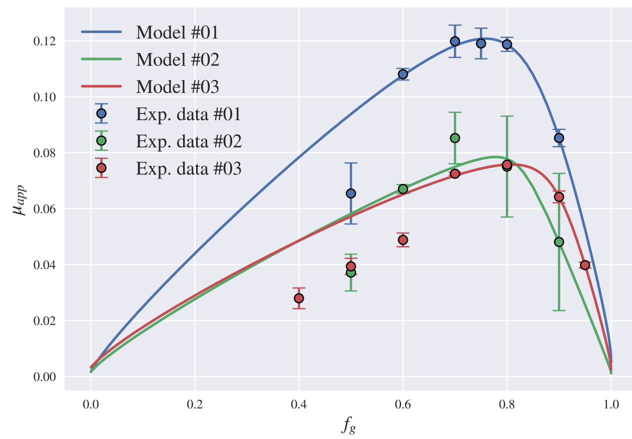


Fig. 3: Experimental data and STARS model evaluations for all the datasets.

Table 5 summarizes the parameter estimates obtained after applying the least-squares method in the three datasets. The parameters $fmmob$, $SF$, and $sfbet$ represent the reference mobility reduction factor, the water saturations around which weak foam collapses, and the sharpness from the transition between low- and high-quality foam regimes. The lower the $sfbet$ value, the smoother the transition from high to low quality, whereas larger values for $sfbet$ represent a sharp transition. The estimated values for $sfbet$ are in good agreement with the transition observed in the experimental data, where datasets #02 and #03 have a more sharp transition than dataset #01. The estimated values for $SF$ for all datasets agree with two decimals places. The estimated values of $fmmob$ for all datasets are again in good agreement with the corresponding data, where for instance, the dataset #01 presents the highest apparent viscosity value among the datasets.

Table 5: STARS parameters estimated with nonlinear least-squares method.

| Dataset / Parameter | $fmmob$ | $SF$ | $sfbet$ |
|---|---|---|---|
| Dataset #01 | 292.71 | 0.44 | 367.88 |
| Dataset #02 | 180.92 | 0.44 | 541.86 |
| Dataset #03 | 173.10 | 0.44 | 419.77 |

ICCS Camera Ready Version 2022
To cite this paper please use the final published version:
DOI: 10.1007/978-3-031-08760-8_26

### 3.2 Foam Model Parameters' Distributions

Next, to better characterize the parameters for each dataset, we performed a Bayesian inference using the MCMC method with the priors given in Table 4. After the execution of the method, the posterior distribution was obtained for each parameter of the model. Figure 4 shows the densities of the parameters of the STARS models, where one can observe that the distributions of $fmmob$ and $SF$ are more concentrated around the mean value, whereas the distribution for $sfbet$ is more spread out and less symmetrical.

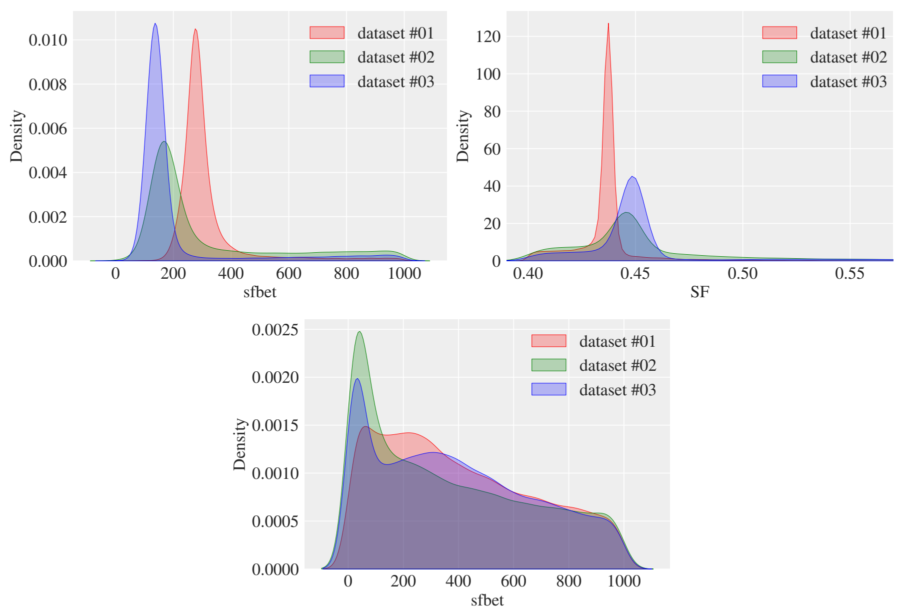


Fig. 4: Posterior distributions for $fmmob$, $SF$, and $sfbet$ parameters of the STARS foam model obtained by the MCMC method.

### 3.3 Forward Uncertainty Quantification Results

Figure 5 shows the propagation of uncertainty for the apparent viscosity for the STARS model. The shaded region represents the prediction interval, the solid lines represent the expected values, and the dots represent the experimental data. Experiment data from datasets #01, #02, and #03 are represented in blue, green, and red, respectively.

Analyzing the result of dataset #01 it is possible to observe that the expected value curves are close to the experimental data. For dataset #02 it is also possible to observe that the expected value curves are close to the experimental data, except when $f_g = 0.5$. The same is true for dataset #03, except for lower values

ICCS Camera Ready Version 2022
To cite this paper please use the final published version:
DOI: 10.1007/978-3-031-08760-8_26

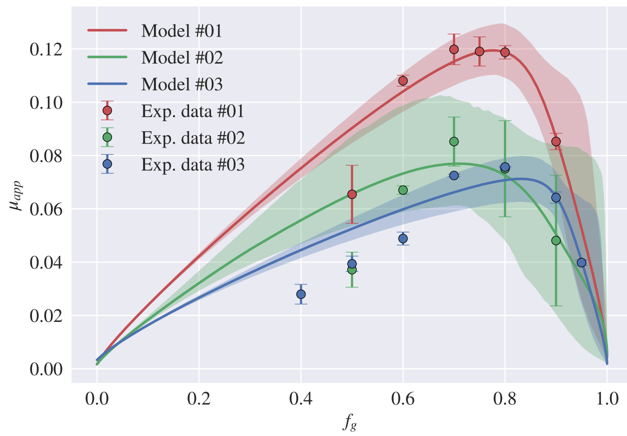


Fig. 5: Uncertainty quantification results of apparent viscosity

of $f_g$. It is also possible to observe that the prediction interval observed in the low-quality regime is smaller than in the high-quality regime.

For dataset #02, the uncertainty range is large, jeopardizing the model's predictions. One hypothesis is that this dataset has a smaller number of data, i.e., the lack of data may have caused it. To confirm this hypothesis, we added two synthetic points generated with a significant random noise: thus, we define a normal distribution with a mean given by the point value obtained by the parameters estimated by the maximum a posteriori (MAP) estimator and a standard deviation of 25% of the MAP estimator around the mean found:

$$\mu_{app} \sim \mathcal{N}\left(\mu_{app}^{\mathrm{MAP}}\left(SF^{\mathrm{MAP}}, fmmob^{\mathrm{MAP}}, sfbet^{\mathrm{MAP}}\right), 0.25 \times \mu_{app}^{\mathrm{MAP}}\right).$$

With this approach the dataset was augmented with the following data:

$$(f_g, \mu_{app}) \approx (0.402, 0.058), (0.970, 0.049).$$

With the modified dataset (experimental and synthetic), we performed inverse UQ using the MCMC method and then forward UQ using the STARS model. The results showed a significant reduction in the range of uncertainties, as presented in Figure 6. Therefore, the hypothesis that the cause of significant uncertainty was due to the lack of data is probably correct.

### 3.4 Sensitivity Analysis

Observing the main and total Sobol indices with respect to apparent viscosity ($\mu_{app}$) for the different datasets, as shown in Figure 7, it is possible to notice that high order interactions between the parameters are negligible. It is also possible

ICCS Camera Ready Version 2022
To cite this paper please use the final published version:
DOI: 10.1007/978-3-031-08760-8_26

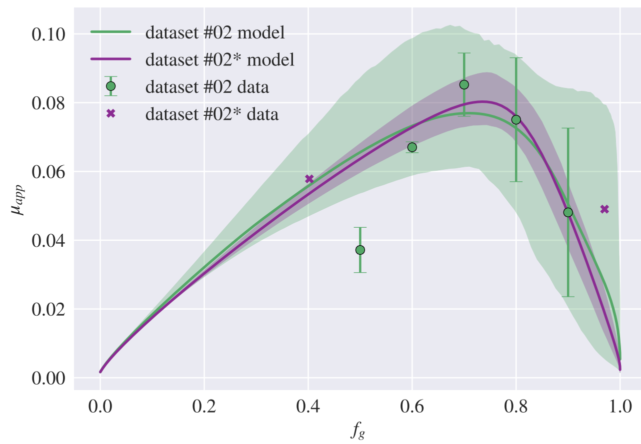


Fig. 6: Forward uncertainty quantification results of apparent viscosity for the augmented dataset.

to observe that $fmmob$ dominates the output variance in the model for high water saturation values. Also, close to the expected value found for $SF$ there is a significant change in its influence and the more uncertainty appears in its PDF (see Figure 4), the larger is the range of $S_w$ that the $SF$ parameter dominates the sensitivity. For values of $S_w$ below this region, the $sfbet$ parameter dominates the sensitivities.

## 4 Conclusions

This work presented a framework for uncertainty quantification and sensitivity analysis of experimental data of core flooding and Bayesian model calibration in foam flow in porous media, referring to a series of three foam quality scans. The mathematical models of foam injection involve many parameters that control the complex physics of this process. The quantification of uncertainties is essential for the development of robust simulators. After performing the model calibration for the experimental data using an inverse Bayesian estimation, the direct UQ analysis for the apparent viscosity showed more significant uncertainties in dataset #02.

The addition of synthetic data made it possible to reduce model uncertainties significantly. In summary, it was possible to conclude through this work that the use of uncertainty quantification and sensitivity analysis contributes to understanding the phenomenon of foam flow in porous media. The use of these tools together can help to confront experiments and models to assess their quality and uncertainties and suggest new experiments to improve the model's reliability.

ICCS Camera Ready Version 2022
To cite this paper please use the final published version:
DOI: 10.1007/978-3-031-08760-8_26

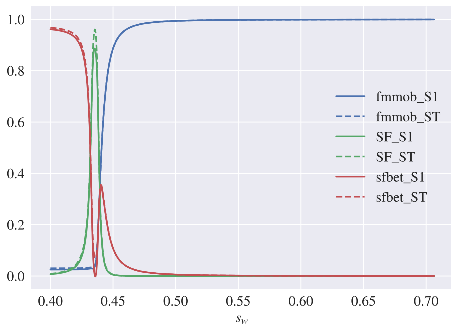


(a) dataset #01

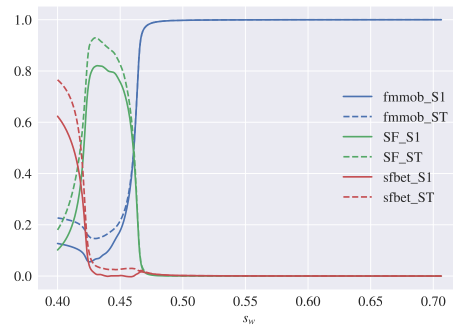


(b) dataset #02

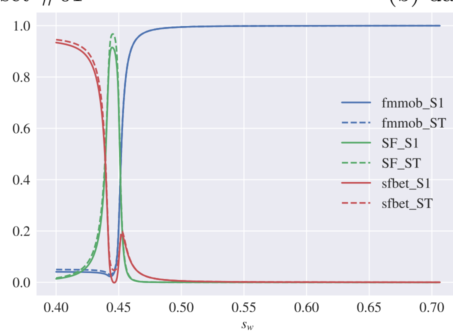


(c) dataset #03

Fig. 7: Sensitivity analysis using main ($S_i$) and total ($S_{T_i}$) Sobol indices for the apparent viscosity.

In the near future, the framework presented in this work will be used on other datasets to perform a more robust validation of the proposed methods and pipeline, which seeks to reduce model uncertainties. In addition, whereas the current work focuses on two-phase experiments, we expect it to be scalable in the sense that the presented pipeline can also be applied to databases of three-phase experiments.

**Acknowledgements** The authors thank Dr. Ivan Landin for suggestions on improving the manuscript.

This research was carried out in association with the ongoing R&D projects ANP number 20358-8, “Desenvolvimento de formulações contendo surfactantes e nanopartículas para controle de mobilidade de gás usando espumas para recuperação avançada de petróleo” (PUC-Rio / Shell Brasil / ANP) and ANP number 201715-9, “Modelagem matemática e computacional de injeção de espuma usa em recuperação de petróleo” (UFJF/Shell Brazil/ANP) sponsored by Shell Brasil under the ANP R&D levy as “Compromisso de Investimentos com Pesquisa e Desenvolvimento”, in partnership with Petrobras.

G.C. was supported in part by CNPq grant 303245/2019-0 and FAPEMIG grant APQ-00405-21. B. M. R. was supported in part by CNPq grant 310722/2021-7.

## References

1. Ashoori, E., Marchesin, D., Rossen, W.: Roles of transient and local equilibrium foam behavior in porous media–traveling wave. In: ECMOR XII-12th European Conference on the Mathematics of Oil Recovery. pp. cp–163. European Association of Geoscientists & Engineers (2010)
2. Berg, S., Unsal, E., Dijk, H.: Non-uniqueness and uncertainty quantification of relative permeability measurements by inverse modelling. Computers and Geotechnics **132**, 103964 (2021)
3. Boeije, C., Rossen, W.: Fitting foam simulation model parameters to data. In: IOR 2013-17th European Symposium on Improved Oil Recovery. pp. cp–342. European Association of Geoscientists & Engineers (2013)
4. Brooks, S.: Markov chain monte carlo method and its application. Journal of the royal statistical society: series D (the Statistician) **47**(1), 69–100 (1998)
5. Chen, Y., Elhag, A.S., Poon, B.M., Cui, L., Ma, K., Liao, S.Y., Reddy, P.P., Worthen, A.J., Hirasaki, G.J., Nguyen, Q.P., et al.: Switchable nonionic to cationic ethoxylated amine surfactants for co2 enhanced oil recovery in high-temperature, high-salinity carbonate reservoirs. SPE journal **19**(02), 249–259 (2014)
6. (CMG)., C.M.G.: Stars users manual; version 2019.10 (2019)
7. Facanha, J.M.d.F., Souza, A.V.O., Gramatges, A.P.: Comportamento de espumas em rochas carbonáticas análogas: comparação com curvas de traçador e efeito da permeabilidade. In: Rio Oil and Gas Expo and Conference. Brazilian Petroleum, Gas and Biofuels Institute - IBP (2020). https://doi.org/10.48072/2525-7579.rog.2020.039
8. Farajzadeh, R., Lotfollahi, M., Eftekhari, A.A., Rossen, W.R., Hirasaki, G.J.H.: Effect of permeability on implicit-texture foam model parameters and the limiting capillary pressure. Energy & Fuels **29**(5), 3011–3018 (2015). https://doi.org/10.1021/acs.energyfuels.5b00248, https://doi.org/10.1021/acs.energyfuels.5b00248
9. Herman, J., Usher, W.: SALib: An open-source python library for sensitivity analysis. The Journal of Open Source Software **2**(9) (jan 2017). https://doi.org/10.21105/joss.00097, https://doi.org/10.21105/joss.00097
10. Kam, S.I.: Improved mechanistic foam simulation with foam catastrophe theory. Colloids and Surfaces A: Physicochemical and Engineering Aspects **318**(1-3), 62–77 (2008)
11. Lotfollahi, M., Farajzadeh, R., Delshad, M., Varavei, A., Rossen, W.R.: Comparison of implicit-texture and population-balance foam models. Journal of Natural Gas Science and Engineering **31**, 184–197 (2016)
12. Ma, K., Lopez-Salinas, J.L., Puerto, M.C., Miller, C.A., Biswal, S.L., Hirasaki, G.J.: Estimation of parameters for the simulation of foam flow through porous media. part 1: the dry-out effect. Energy & fuels **27**(5), 2363–2375 (2013)
13. Mohamed, I., Nasr-El-Din, H., et al.: Formation damage due to co2 sequestration in deep saline carbonate aquifers. In: SPE International Symposium and Exhibition on Formation Damage Control. Society of Petroleum Engineers (2012)

ICCS Camera Ready Version 2022
To cite this paper please use the final published version:
DOI: 10.1007/978-3-031-08760-8_26

14. Newville, M., Stensitzki, T., Allen, D.B., Rawlik, M., Ingargiola, A., Nelson, A.: Lmfit: Non-linear least-square minimization and curve-fitting for python. Astrophysics Source Code Library pp. ascl–1606 (2016)
15. Salvatier, J., Wiecki, T.V., Fonnesbeck, C.: Probabilistic programming in python using pymc3. peerj computer science, 2, e55 (2016)
16. Valdez, A.R., Rocha, B.M., da Fonseca Facanha, J.M., de Souza, A.V.O., Perez-Gramatges, A., Chapiro, G., dos Santos, R.W.: Foam-assisted water–gas flow parameters: From core-flood experiment to uncertainty quantification and sensitivity analysis. Transport in Porous Media pp. 1–21 (2021)
17. Valdez, A.R., Rocha, B.M., Chapiro, G., dos Santos, R.W.: Uncertainty quantification and sensitivity analysis for relative permeability models of two-phase flow in porous media. Journal of Petroleum Science and Engineering **192**, 107297 (2020)
18. Zeng, Y., Muthuswamy, A., Ma, K., Wang, L., Farajzadeh, R., Puerto, M., Vincent-Bonnieu, S., Eftekhari, A.A., Wang, Y., Da, C., et al.: Insights on foam transport from a texture-implicit local-equilibrium model with an improved parameter estimation algorithm. Industrial & Engineering Chemistry Research **55**(28), 7819–7829 (2016)
19. Zitha, P., Du, D.: A new stochastic bubble population model for foam flow in porous media. Transport in Porous Media **83**(3), 603–621 (2010)

ICCS Camera Ready Version 2022
To cite this paper please use the final published version:
DOI: 10.1007/978-3-031-08760-8_26